Condensed Matter Physics 2010, Vol. 13, No 4, 43401: 1–7

http://www.icmp.lviv.ua/journal

CONDENSED MATTER PHYSICS

Initial conditions for turbulent mixing simulations

T. Kaman[1], J. Glimm[1,2], D.H. Sharp[3]

[1] Department of Applied Mathematics and Statistics, Stony Brook University, Stony Brook, NY 11794–3600, USA

[2] Computational Science Center, Brookhaven National Laboratory, Upton, NY 11793–6000, USA

[3] Los Alamos National Laboratory, Los Alamos, NM 87545, USA

Received June 23, 2010

In the context of the classical Rayleigh-Taylor hydrodynamical instability, we examine the much debated question of models for initial conditions and the possible influence of unrecorded long wave length contributions to the instability growth rate α.

Key words: *turbulent mixing layers, turbulent diffusion*

PACS: *47.27.wj, 47.27.tb, 47.27-i*

1. Introduction

Turbulent mixing has been a challenge for sixty years, attracting the talents of leading physicists and mathematicians. Recently we have proposed a new LES algorithm, [1, 2] based on Front Tracking [3, 4] (to control unphysical numerical diffusion of species mixture) and subgrid scale (SGS) models to regularize the effects of the unresolved scales, as they influence the resolved ones [5]. We have success with matching simulation with experiment according to the following criteria:

- simulation agreement with 14 different experiments [2, 6–8],
- agreement with sufficient accuracy (often) to distinguish between distinct experiments [8],
- agreement for both immiscible and miscible experiments, the latter for high, moderate and low Schmidt number [8, 9],
- agreement both where initial conditions were recorded (and used to initialize the simulation) and where they were not [8],
- agreement with other simulations in one of the few cases where simulation-experiment agreement was achieved by others [8].

We have presented numerical evidence that the mixing rate α is nonuniversal, in that it depends on at least six nondimensional groups [9]. It depends on long wave contributions to the initial interface perturbation, as is generally acknowledged, and has been shown by others. We show that α also depends on two dimensionless characterizations of the short wave initial conditions, namely the ratios of the maximally unstable wave length $\lambda = \lambda_c$ and of the thickness of the initial diffusion layer to the dominant short wave length perturbation. We also show that it depends on the fluid transport properties (Schmidt, Prandtl and Grashof numbers) [8, 9]. Here the maximally unstable wave length λ_c comes from the theory of dispersion relations. Dispersion theory is a theoretical solution of the Rayleigh-Taylor instability problem, linearized for small perturbation amplitudes; its solution is a growth rate as a function of wave length. The mixing rate α is defined in terms of the penetration distance h of the light fluid into the heavy fluid ("bubbles"), via the formula

$$h = \alpha A g t^2, \tag{1}$$

where g denotes the acceleration of a fluid discontinuity and the Atwood number is a dimensionless measure of the density contrast between the two fluids, $A = (\rho_2 - \rho_1)/(\rho_2 + \rho_1)$.

The ongoing debate over α centers on initial conditions and can perhaps be summarized as follows:

(i) Fourier spectral amplitudes $A(k)^2 \sim k^{-2}$ and k^{-3} have been proposed for the initial perturbations to yield the growth law (1) based on superposition of modes, nonlinear single mode RT growth rates of the Fourier modes, and saturation of this growth at larger amplitudes [10, 11]. The difference between the two proposed exponents for the spectral amplitudes has to do with the lumping of modes for adjacent frequencies k into a single effective mode.

(ii) Given that long wave length perturbations do influence the growth rate α, how can valid experimental-simulation comparisons be achieved for experiments for which these initial conditions were not recorded?

(iii) In the high Re limit, dependence on nonuniversal fluid parameters such as the Schmidt number should disappear, and then α becomes universal, other than its dependence on initial conditions.

(iv) Many simulation codes achieve growth rates with an α as in (1) half or less than the experimentally observed values when initialized without long wave length perturbations. Consensus of simulation codes has been claimed as an indication of scientific truth.

The first goal of this paper is to examine the k^{-3} or k^{-2} hypothesis of (i) in the context of experimental data [12, 13]. We find evidence for a negative exponent, $A^2 \sim k^{-a}$, $a \approx 4$ at the initial time. We note a strong time dependence for the relative spectral amplitudes, with $A^2 \sim k^0$ at the early time (third plate) plot, and the fraction of long wave spectral energy dropping from 50% to 80% initially to about 2% at the time of the third plate. k^{-2} and $k^{-3/2}$ A^2 initial spectra have been observed in the machined surfaces present in plasma experiments [14]. The second purpose of this paper is to develop a plan for use of experimental data in simulation initialization.

Concerning (iii), our validation-simulation tests [8] show a 20% decrease in α as Sc changes from 560 to 1 at $Re = 40,000$, thus documenting a nonuniversal and Sc dependent α well above the transition value $Re = 10,000$ sometimes cited as a universal Reynolds number for the rapid transition to hard turbulence.

Item (iv) was previously discussed [8, 9]. Briefly, most RT simulations neglect the influence of numerical mass diffusion and of the six dimensionless groups which have been shown to influence the value of α, beyond the fact that the argument in (iv) is prima facie weak, and generally not acceptable as a basis for scientific conclusions.

2. Scaling laws for initial perturbation amplitudes

The essence of our approach for determining experimental initial perturbations is to transfer information from the experimentally observed early time RT experimental photographs to time $t = t_0 = 0$. We start by measuring the locations of all bubble minima in the third experimental plate. As is standard in the analysis of these experiments, the edge (corner) bubbles are not included as they have an exceptional amplitude. For confirmation purposes, we also record the bubble minima in the second experimental plate where they are clear enough to be reliable (experiment #105 [13]), or in the fourth plate when the second plate is not clear (#56 and #63 [12] and #104, #114 [13]). The bubble minima heights are Fourier analyzed, giving Fourier amplitudes as a function of wave number n. The mode $n = 0$ represents the mean bubble position, and it is clearly the dominant short wave length datum. The other modes can be regarded as long and short wave length perturbations of this dominant signal. These other modes are generally of small amplitude and (especially if the methodology of (i) is to be accepted), have a time evolution governed by superposition of the propagation of single mode solutions for the RT fluid equations. The linear propagation is based on the theory of dispersion relations, which defines an exponential growth

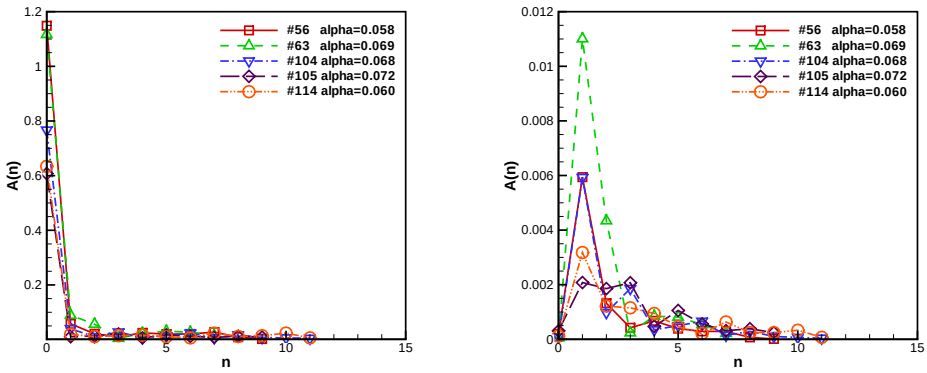

Figure 1. Left: measured values for the spectral amplitude at $t = t_3$. Right: $t = t_0$ inferred spectral amplitudes $A(n)$ (cm) for the bubble minima for several experiments [12, 13] vs. n. Here and below, wave numbers are cut off at the Nyquist value $n_{\max}/2$.

rate. Using this theory, we transfer time t_j mode amplitudes back to time t_0, where t_j denotes the time of the j^{th} plate, for $j \geqslant 1$. The criteria for choosing linear vs. nonlinear single mode propagation is based on the ratio of wave length to amplitude, and as this is ratio not too large, the simpler linear theory is used.

The mode $n = 0$ is assigned the most rapid growth rate, as it represents the dominant bubble size. Since this mode is never small at the time of the third experimental plate, we proceed differently in this case. The maximum bubble location has been recorded experimentally, and we start from the earliest of these recorded values for the backward in time propagation of the $n = 0$ mode. There is a difference between the mean bubble height, referred to here, and the maximum bubble height, as recorded experimentally. In previous analysis of the same data as considered here [15], we observed a time independent ratio for the maximum to mean bubble height. Using this ratio, we infer the mean bubble height at the earliest recorded time. Using this mean bubble minima at this time, we find that the height to wave length ratio allows propagation back to time $t = t_0$ by linear RT single mode analysis. See figure 1.

To split the $t = t_0$ or $t = t_j$ modes into long and short wave lengths, we combine the $n = 0$ and the collective short wave length signal into a combined short wave length mode and we combine the rest into a long wave length signal. The wave length interval $[\frac{2}{3}\lambda_c, \frac{4}{3}\lambda_c]$ comprises the short wave length spectrum. Using the relation $n = L/\lambda$ where $L = 15$ for all experiments considered here, the short wave number n interval is $[3L/4\lambda_c, 3L/2\lambda_c]$. Larger n values, if any, are included in the short wave length spectrum, as is the $n = 0$ value. The smaller n values (other than $n = 0$) describe the long wave length perturbation, often referred to as "long wave length noise". The long wave length spectrum comprises most of figure 1, in the region to the left, other than the $n = 0$ value.

The assessment (i) comes from plotting the long wave length data only, with log-log scaled coordinates. In the log-log plot, see figure 2, the exponent of n is the slope of the data. There is over a decade of long wave length n values, sufficient for the approximate determination of the slope, but the noise in the data only allows an approximate assessment of the spectral exponent, $A(n)^2 \sim n^{-a}$, $a \approx 4$. The power law with amplitudes $A(n)^2 \sim n^{-a}$, $a = 2$ or $a = 3$ has been mentioned especially, as, if substituted into a dispersion relation growth rate, with a cut off in growth at a saturation amplitude $A \approx \lambda$, a Rayleigh-Taylor growth rate $h \sim Agt^2$ can be obtained through a purely theoretical argument. The exponent a is, however, strongly time dependent, and for most of the experimentally self similar mixing regime, it is close to zero. See table 1. Thus the theory that the observed self similar RT growth rates can be determined from the long wave length perturbations in the initial data is inconsistent with the experimental data. The alternate

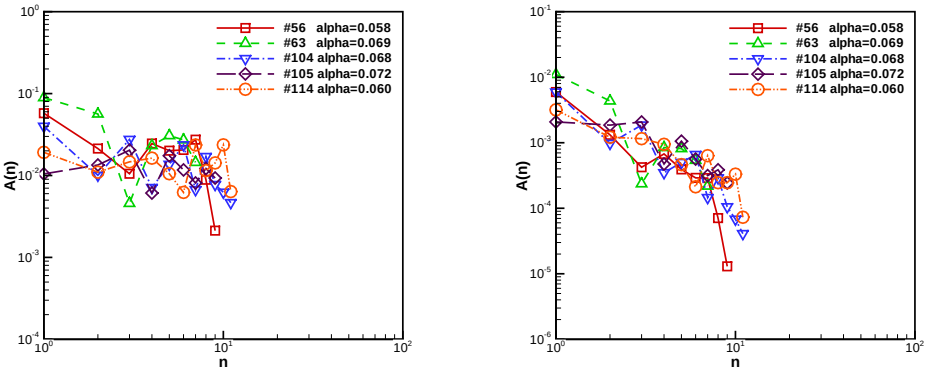

Figure 2. Log-log plot of amplitudes vs. wave number, excluding $n = 0$, inferred at $t = t_0$. This data satisfies a power law $A(n)^2 \sim n^{-a}$, $a \approx 4$. Left: measured data from $t = t_3$. Right: inferred data for $t = t_0$.

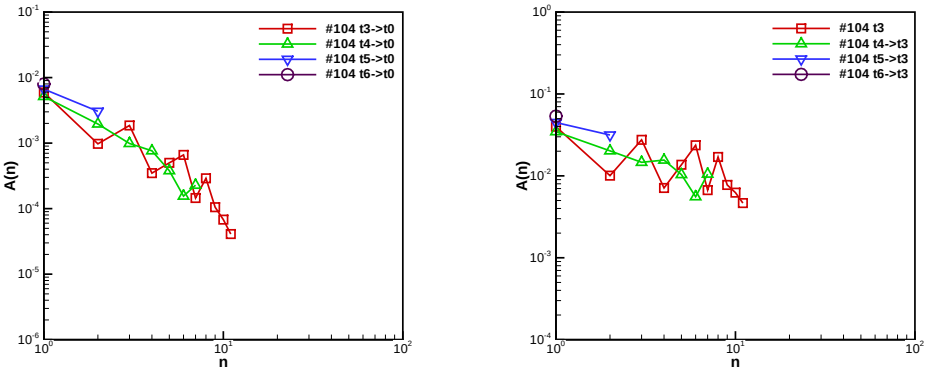

Figure 3. Log-log plot of amplitudes vs. wave number, excluding $n = 0$, from experiment #104. Left: predictions of $t = t_0$ data starting from different times $t = t_j$. Right: Prediction of the measured $t = t_3$ data starting from different $t = t_j$.

explanation of RT growth as due to bubble merger [15] remains the only theoretical explanation for the observed RT growth rates that is consistent with experimental data. To assess the accuracy of this time transfer of spectral amplitudes, we use the method to predict the results with known data, and we use it to predict the same unknown data, but from different starting times, see figure 3.

3. Initialization of RT simulations

The second purpose of this paper is to construct initial conditions for new RT simulations that reflect experimental initial conditions. Thereby, we address item (ii).

Carrying out the transfer of spectral amplitudes from $t = t_3$ to $t = t_0$, we have spectral amplitudes and relative amplitudes for the long wave length perturbation, at the time of the third experimental plate (directly observed), and at an experimental or simulation initial time. We introduce the L_2 norms squared (spectral energies) $L^2 = A^2_{\text{long}}$ and $S^2 = A^2_{\text{short}}$ of the long and short wave length portions of the Fourier spectrum. Also we define T and R: $T^2 = L^2 + S^2$ and $R^2 = L^2/T^2$. To specify the normalization, we define $L^2 = A^2_{\text{long}} = \sum_{k,\text{long}} A(k)^2$.

Table 1. Spectral exponents for A^2 at experimental initial and recorded data times.

Exp.	#56 [12]	#63 [12]	#104 [13]	#105 [13]	#114 [13]
$t_{3,0}$	–4.5	–4.1	–4.3	–3.0	–3.8
$t_{4,0}$	–3.9	–3.6	–4.3	–3.6	–3.6
$t_{5,0}$	–4.0	–3.2	–4.0	–3.6	–3.0
$t_{3,1}$	–2.5	–2.3	–3.6	–2.8	–2.7
$t_{3,2}$	–1.4	–1.3	–1.7	–0.9	–1.6
t_3	–0.4	–0.2	–0.4	–0.1	–0.4
t_4	–0.3	–0.4	–0.2	–0.2	–0.1
t_5	–0.5	–0.1	–0.2	–0.3	–0.4

Table 2. Long and short wave length spectral energies, observed directly at $t = t_3$ and t_2 or t_4, and inferred/confirmed from this data for $t = t_0$. Also shown is the relative difference Δ in these two inferences for $t = t_0$ data. Experiments #56 and #104 had an apparent small amplitude long wave length perturbation from visual observation of the data, while #63 was vibrated mechanically to induce a long wave length perturbation. Experiments #105 and #114 had no experimentally noted long wave length nor was any detectable from examination of the early time plates.

Exp.	#56 [12]	#63 [12]	#104 [13]	#105 [13]	#114 [13]
$L^2_{t_3}$	0.022	0.031	0.010	0.0058	0.0054
$S^2_{t_3}$	1.152	0.977	0.551	0.334	0.422
$T^2_{t_3}$	1.174	1.008	0.561	0.339	0.427
$R^2_{t_3}$	0.019	0.031	0.018	0.017	0.0125
$R^2_{t_4}$	0.067	0.058	0.0224	0.009	0.0128
$R^2_{3,0}$	0.998	0.9999	0.9997	0.947	0.998
$R^2_{4,0}$	0.999	0.9999	0.9996	0.939	0.995
ΔR^2_0	0.001	0.0000	0.0001	0.008	0.003

In table 2, we present the related L_2 norms squared (spectral energies) for the rocket rig data. We define $L^2_{t_j}$ as the long wave length L_2 norm squared as measured and Fourier analyzed for $t = t_j$, $j = 3, 4$. We infer $t = t_0$ spectral energies from those at $t = t_3$. All data obtained from $t = t_3$ is confirmed by an independent analysis using $t = t_4$ data and $t = t_2$ data where possible. These inferred spectral energies are labeled $L^2_{j,0} = L^2_{t_j \to t_0}$. We define similar short wave length and total spectral energies S^2 and T^2 and ratios R^2. As a justification for these constructions, we compare the differences in the $R^2_{j,0}$, defining $\Delta R^2_0 = |R^2_{3,0} - R^2_{4,0}|$, or a similar expression using $t = t_2$ data if available. It is interesting to note the striking decrease in the long wave relative long wave length spectral energy R^2 from $t = 0$ to $t = t_3$.

Conventional initialization of Rayleigh-Taylor mixing is to use uniform amplitudes over the short wave length interval with random phases. This can be referred to as "ideal random initial conditions". At the time $t = t_3$ of the third experimental plate, the observed wave length for the experiments #104, #105, #114 is approximately equal to λ_c, indicating that no mode doubling has occurred at this time. The observed wave length at the time $t = t_3$ for experiments #56 and #63 is about two times λ_c, indicating one round of mode doubling has occurred at the time $t = t_3$.

The Fourier modes (especially the long wave length ones in the above sense) can be used to provide an improved initialization. We propose to use the inferred long wave length Fourier amplitudes and phases at a $t_{\text{sim}} = 0$, with t_{sim} defined through limiting the fastest growing mode to small amplitude. These amplitudes will be combined with an ideal short wave length perturbation as initialization, with the relative amplitudes of the two governed by the ratios computed as in table 2. This construction yields data for only one of the required two dimensions for initialization.

Table 3. Simulation-experiment comparisons for various experiments. The wave length in column 3 (units cm) comes from dispersion relations in which all physical transport parameters are used.

Ref.	#	λ_c (cm)	α_{exp}	α_{sim}
[12]	#56	0.27	0.058	0.070
[12]	#63	0.27	0.069	0.070
[13]	#104	0.43	0.068	0.070
[13]	#105	0.46	0.072	0.070
[13]	#114	0.44	0.060	0.070

The other horizontal direction, not visible in the experimental plates, has one third the size of the visible direction, 5 cm vs. 15 cm. Thus the experiment does not allow for long wave length perturbations in this direction, and only marginally allows medium length perturbations outside the range of the ideal short wave length perturbations. We propose to choose an ideal short wave length initialization in this direction.

The simulation results in the last column of table 3 were performed with ideal random initial conditions. The most unstable wave length λ_c, which determines these initial conditions, was set by dispersion relations using surface tension alone, i.e. without corrections due to viscosity. It is for this reason that one simulation [6] is used to model all the experiments in table 3.

As we prepare to repeat the simulations of [6], we propose to:

- determine λ_c from complete physics (use of distinct viscosities in the two fluids) to contribute to the setting of the length scale for the ideal random short wave length initial conditions,
- use the inferred long wave length perturbations to set amplitude and phases for the long wave length perturbations in the observed direction combined with ideal short wave length perturbations in both directions,
- use laminar and turbulent viscosity of the experimental fluids with an LES simulation with dynamic subgrid models.

In conclusion, we have shown that the power law $A(n)^2 \sim n^{-a}$, $a \approx 4$, is consistent with experimental data. We have shown a striking decrease in the long wave length portions of the spectral energies from 99% initially to about 1% after the first observable times and a decrease in the negative spectral power law exponent from $a \approx -4$ to $a \approx -0.3$. Thereby, the long wave length initial spectra does not play an important role in the experimentally observed self similar scaling law for α. We have developed a plan for a UQ study of α related to uncertainty in initial conditions.

Acknowledgements

It is a pleasure to thank D. Youngs for helpful comments and for sharing unpublished experimental data. This research was supported in part by the U.S. Department of Energy grants DE–FC02–06–ER25770, DE–FG07–07ID14889, DE–FC52–08NA28614 and DE–AC07–05ID14517. This work is supported by the Army Research Organization grant W911NF0910306. This manuscript has been co-authored by Brookhaven Science Associates, LLC, under Contract No. DE–AC02–98CH10886 with the U.S. Department of Energy. The United States Government retains, and the publisher, by accepting this article for publication, acknowledges, a world-wide license to publish or reproduce the published form of this manuscript, or allow others to do so, for the United States Government purposes. This work has a Los Alamos Laboratory preprint number LA–UR 10–03424 and a Stony Brook University preprint number SUNYSB–AMS–10–03.

References

1. Lim H., Yan Y., Glimm J., Sharp D.H., High Energy Density Physics, 2010, **6**, 223; Preprint of the Stony Brook University: SUNYSB–AMS–09–02; Preprint of the Los Alamos National Laboratory: LA–UR–09–01364.
2. Lim H. et al., Physica Scripta, 2009 (submitted for publication); Preprint of the Stony Brook University: SUNYSB–AMS–08–07; Preprint of the Los Alamos National Laboratory: LA–UR–08–07725.
3. Du J. et al., J. Comput. Phys., 2006, **213**, 613.
4. Glimm J. et al., SIAM J. Sci. Comp., 1998, **19**, 703.
5. Moin P., Squires K., Cabot W., Lee S., Phys. Fluids, 1991, **A3**, 2746.
6. George E., Phys. Rev. E, 2006, **73**, 016304.
7. Liu X.F., George E., Bo W., Glimm J., Phys. Rev. E, 2006, **7**3, 056301.
8. Lim H., Iwerks J., Glimm J., Sharp D.H., PNAS, 2010; Preprint of the Stony Brook University: SUNYSB–AMS–09–05; Preprint of the Los Alamos National Laboratory: LA–UR–09–06333.
9. Lim H. et al., Physica Scripta, 2009 (in press); Preprint of the Stony Brook University: SUNYSB–AMS–09–07; Preprint of the Los Alamos National Laboratory: LA–UR–09–07240.
10. Dimonte G., Phys. Rev. E, 2004, **69**, 056305.
11. Youngs D.L., American Institute of Aeronautics and Astronautics, Technical report 4102, 16th AIAA Computational Fluid Dynamics Conference, 2003.
12. Burrows K.D., Smeeton V.S., Youngs D.L., AWE report number 0 22/84, 1984.
13. Smeeton V.S., Youngs D.L., AWE report number 0 35/87, 1987.
14. Barnes C. et al., Phys. Plasmas, 2002, **9**, 4431.
15. Cheng B., Glimm J., Sharp D.H., Chaos, 2002, **12**, 267.

Початкові умови для моделювання турбулентного змішування

Т. Каман[1], Дж. Глімн[1,2], Д.Г. Шарп[3]

[1] Факультет прикладної математики і статистики, Університет Стоні Брук, Стоні Брук, США

[2] Науковий обчислювальний центр, Національна лабораторія Брукхейвена, Уптон, США

[3] Лос Аламоська національна лабораторія, Лос Аламос, США

У контексті класичної гідродинамічної нестійкості Релея-Тейлора ми вивчаємо дуже дискусійне питання моделей для початкових умов і можливий вплив незафіксованих далекосяжних вкладів на швидкість росту нестійкості α.

Ключові слова: *шари турбулентного змішування, турбулентна дифузія*